

Influences of the magnetic coupling process on the spectrum of a disk covered by the corona

R.-Y. Ma, D.-X. Wang, and X.-Q. Zuo

Department of Physics, Huazhong University of Science and Technology, Wuhan 430074, PR China
e-mail: dxwang@hust.edu.cn

Received 23 September 2005 / Accepted 23 January 2006

ABSTRACT

Context. Recently, much attention has been paid to the magnetic coupling (MC) process, which is supported by the very high emissivity indexes observed in Seyfert 1 galaxy MCG-6-30-15 and GBHC XTE J1650-500. But the rotational energy transferred from a black hole is simply assumed to be radiated away from the surrounding accretion disk in the black-body spectrum, which is obviously not consistent with the observed hard power-law X-ray spectra.

Aims. We introduce a corona into the MC model to make it more compatible with observations.

Methods. We describe the model and the procedure of a simplified Monte Carlo simulation, compare the output spectra in the cases with and without the MC effects, and discuss the influences of the three parameters involved in the MC process on the output spectra.

Results. It is shown that the MC process augments radiation fluxes in the UV or X-ray band. The emergent spectrum is affected by the BH spin and magnetic field strength at the BH horizon, while it is almost unaffected by the radial profile of the magnetic field at the disk.

Conclusions. Introducing corona into the MC model will improve the fitting of the output spectra from AGNs and GBHCs.

Key words. accretion, accretion disks – black hole physics – magnetic fields

1. Introduction

Tenuous hot plasma (corona) is commonly believed to exist in the inner region of the accretion flow, which is produced and heated by magnetic activities, such as reconnection and flare (e.g. Liang & Price 1977; Galeev et al. 1979). The influences of the disk corona on the emergent spectrum from active galactic nuclei (AGNs) and galactic black-hole candidates (GBHCs) have been discussed by many authors: e.g. Haardt & Maraschi (1991, hereafter HM91; 1993), Field & Rogers (1993), Esin (1999), Zhang et al. (2000), and Liu et al. (2002). A corona explains the power-law X-ray spectra very well, and reprocessing of the coronal X-rays by cold disk gives rise to the observed emission lines naturally, in which the iron $K\alpha$ fluorescence line provides a diagnostic of both the geometry of the accretion flow and the property of the spacetime around the black hole (BH). However, only the gravitational energy of the accreting matter has been invoked to heat the disk and its corona in previous works.

Recently, much attention has been paid to the magnetic coupling (MC) process in which energy is transferred from a rotating BH to its surrounding disk (Blandford 1999; van Putten 1999; Li & Paczynski 2000; Li 2002a; Wang et al. 2002; Wang et al. 2003a,b, hereafter W03a and W03b, respectively), which is in fact a variant of the Blandford-Znajek (BZ) process. The existence of the MC process has been supported by the very high-emissivity indexes observed in Seyfert 1 galaxy MCG-6-30-15 and the GBHC XTE J1650-500, which cannot be explained by the standard accretion disk (Wilms et al. 2001; Miller et al. 2002; Li 2002b).

However, in the previous MC models all the energies that deposit on the disk, both the gravitational energy of the accreting

matter and the rotational energy transferred from the BH, are simply assumed to be radiated away in a black-body spectrum, which is obviously not consistent with the observed hard power-law X-ray spectra. In this paper we intend to introduce corona into the MC model and then discuss the spectrum affected by this MC process. It is shown that the MC process augments the radiation fluxes, while a corona makes MC model more reasonable and more consistent with the observations than was the previous MC model.

The paper is arranged as follows: Sect. 2 gives the description of our model. Section 3 shows the procedure and results of our simplified Monte Carlo simulation, and in Sect. 4 we discuss the applications of our model to observations. Throughout this paper the geometric units $G = c = 1$ are used.

2. Description of our model

The poloidal profile of the large-scale magnetic field and the geometry of the corona are illustrated in Fig. 1. The central BH is fast rotating and surrounded by an axisymmetric magnetosphere. It is assumed that the disk is geometrically thin and optically thick, while the corona is geometrically thick and optically thin. The poloidal magnetic field is assumed to be constant on the horizon and it varies as a power-law with the radial coordinate on the disk, i.e.,

$$B_H = \text{const.}, \quad B_D \propto r^{-n}. \quad (1)$$

In Fig. 1 the angle θ_M indicates the angular boundary between the open and closed field lines at the BH horizon, which can be determined by the mapping relation derived in W03b. Angle θ_L is the lower angular boundary of the closed field lines, and it is supposed to be less than 0.5π to avoid the singularity of the

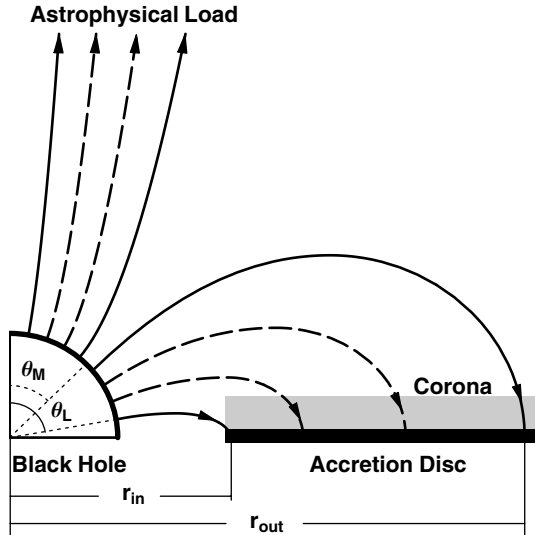


Fig. 1. Poloidal profile of the large-scale magnetic field and the geometry of corona.

closed field lines at the equatorial plane. The magnetic field powers the jet via the BZ process and transfers energy between the BH and the disk via the MC process.

Both large- and small-scale magnetic fields are involved in our model, although the latter is not shown in Fig. 1. The large-scale magnetic field plays a key role in transferring energy and angular momentum from a fast-rotating BH to its surrounding disk or remote astrophysical load in the MC or BZ processes, respectively. The small-scale magnetic field energizes the corona above the disk by virtue of some physical processes, such as magnetic reconnection and buoyancy (HM91). Moreover, the large-scale field can be produced from the small-scale field created by dynamo processes (e.g. Tout & Pringle 1996). Livio et al. (1999) argue that the strength of the large-scale field threading a black hole is very weak if the field is created in the thin disk, because the ratio of the large-scale field to the small-scale field is $\sim H/R \ll 1$, where H is the disk thickness and R the radial size of the field. This greatly confines the BZ and MC powers. Since the thickness of the corona is about the radius of the disk, the large-scale magnetic fields created by dynamo processes in the corona are significantly stronger than those in the thin disk (Cao 2004), and the strong BZ and MC powers are maintained. For simplicity, we suppose that these two kinds of magnetic fields exist independently.

The energy deposited in the corona and disk consists of two parts: (i) the gravitational energy of the accreting matter and (ii) the rotational energy of the BH transferred in the MC process. Some authors (e.g. HM91; Merloni & Fabian 2002) have mentioned physical processes in which the gravitational energy converts to the thermal energies of the corona and disk. However, nobody has proposed any mechanism yet to describe how the rotational energy of the BH transferred in the MC process dissipates. In this paper, we deal with this issue based on the following two considerations.

(i) Based on BH magnetosphere theory (Macdonald & Thorne 1982; Thorne et al. 1986; Li 2002a; W03a), the disk can be regarded as an electromotive force (EMF) in an equivalent circuit due to its rotation, which is opposite to the BH EMF. If the angular velocity of the BH is greater than that of the disk, Poynting flux would flow from the BH to the disk

(W03b). Although the disk is commonly supposed to be a perfect conductor, its interior resistance may not be zero. Part of the MC power may heat the disk, just as Poynting flux gets into the resistance and heats it in a circuit;

(ii) The flux of the angular momentum transferred magnetically from the BH to the disk decreases rapidly with disk radius (see Eq. (3) below), which results in the differential rotation of the accreted matter. Thus the electromagnetic energy converts to thermal dissipation, just as the gravitational energy of accreting matter converts to thermal dissipation in disk accretion.

Detailed discussions of these physical processes are beyond the scope of this paper, and we assume that both the gravitational energy of the disk and the rotational energy of the BH can dissipate into the thermal energy of the corona and disk.

The scenario of the emergent spectrum is described as follows. Thermal soft-seed photons are emitted from the disk. When they cross the rarefied hot corona, some may go through the corona directly without being scattered, some may escape after one or several times of scattering, and others may be down-scattered to the disk by the corona. The fate of the X-ray photon that returns to the disk critically depends upon its energy E : (a) if $E > 100$ keV, the photon loses its energy by Compton recoil; (b) if $E < a$ few keV, the photon is absorbed by ionization or free-free absorption; and (c) it may be both Compton scattered and bound-free absorbed for a few keV $< E < 100$ keV (Field & Rogers 1993). Bound-free absorption or ionization results in a vacancy in the inner shell of an atom, which then leads to a fluorescence photon or the ejection of an Auger electron (for details see George & Fabian 1991, hereafter GF91). Unscattered photons form the component of the UV/soft X-ray band, and photons escaping the corona after inverse Compton scatterings constitute the power-law X-ray spectrum, while photons reprocessed by the disk produce fluorescence lines and a reflection hump.

Here we neglect cyclo-synchrotron radiation since it is less important than Compton radiation in the slab corona (Di Matteo et al. 1997; Ghisellini et al. 1998). We also neglect the bremsstrahlung radiation, assuming that the corona is tenuous enough.

From the above scenario it can be found that part of the energy dissipated in the corona is conveyed to the disk via hard X-rays, i.e., the disk is heated by three kinds of energies: (1) gravitational energy of the accreting matter, (2) rotational energy of the BH transferred to the disk, and (3) the absorbed energy of X-rays coming from the corona. Since the energy of the X-rays eventually comes from the gravitational and rotational energies, we suppose that the fraction of the total energy dissipated in the disk is η , which includes the contribution of the downward X-rays. As shown in HM91, the soft emission is almost only derived from absorption and reprocessing of the high-energy flux impinging on the disk. Roughly half of the Comptonized photons in the corona irradiate and heat the disk, and the other half radiates away, so we take $\eta = 0.5$ in our calculations.

For simplicity in the simulation, the disk is assumed to be “cold”, with hydrogen and helium fully ionized, but all other elements neutral or weakly ionized. Moreover, the energetic and spatial distributions of free electrons in the corona are postulated to be thermal and homogeneous.

3. Simulation of the disk spectrum

3.1. Multicolor black-body spectrum of the disk affected by the MC process

Based on the conservation laws of mass, angular momentum, and energy, the local radiation flux from the disk around a rotating BH is given by Page & Thorne (1974) and Li (2002a),

$$F = \frac{\dot{M}_D}{4\pi r} f + \left(-\frac{d\Omega_D}{r dr} \right) (E^+ - \Omega_D L^+)^{-2} \int_{r_{\text{ms}}}^r (E^+ - \Omega_D L^+) H r dr, \quad (2)$$

where \dot{M}_D , Ω_D , r_{ms} , E^+ , and L^+ are, respectively, the accretion rate, the angular velocity of the disk, the radius of the marginally stable orbit, the specific energy, and angular momentum at the disk radius r . Function f is related to the radiation flux due to disk accretion, and H is the flux of angular momentum transferred between the BH and the disk (W03a),

$$H(a_*, \xi, n)/H_0 = \begin{cases} A(a_*, \xi) \xi^{-n}, & 1 < \xi < \xi_{\text{out}} \\ 0, & \xi > \xi_{\text{out}} \end{cases}, \quad (3)$$

$$A(a_*, \xi) = \frac{a_*(1-\beta)}{2\pi [2 \csc^2 \theta - (1-q)]} \times \sqrt{\frac{1 + a_*^2 \chi_{\text{ms}}^{-4} \xi^{-2} + 2a_*^2 \chi_{\text{ms}}^{-6} \xi^{-3}}{1 - 2\chi_{\text{ms}}^{-2} \xi^{-1} + a_*^2 \chi_{\text{ms}}^{-4} \xi^{-2}}}, \quad (4)$$

where $H_0 \equiv (B_{\text{H}}^p)^2 M$, β is the ratio of the angular velocity of the disk to that of the BH (i.e. $\beta \equiv \Omega_D/\Omega_{\text{H}}$), $\xi = r/r_{\text{ms}}$ is a radial parameter of the disk defined in terms of r_{ms} , and $\chi_{\text{ms}} \equiv \sqrt{r_{\text{ms}}/M}$.

The relation between the magnetic field and the accretion rate is given by Moderski et al. (1997) based on the balance between the pressure of the magnetic field on the horizon and the ram pressure of the innermost parts of an accretion flow

$$(B_{\text{H}}^p)^2/(8\pi) = P_{\text{ram}} \sim \rho c^2 \sim \dot{M}_D/(4\pi r_{\text{H}}^2), \quad (5)$$

where r_{H} is the radius of the horizon. From Eq. (5) we can define $F_0 \equiv (B_{\text{H}}^p)^2 = 2\dot{M}_D/[M^2(1 + \sqrt{1 - a_*^2})^2]$.

For the presence of corona, the dissipated power in the unit area of the disk, F_{d} , is related to $F(r)$ by

$$F_{\text{d}}(r) = \eta F(r), \quad (6)$$

where $F(r)$ is the local radiation flux expressed by Eq. (2). According to the Stefan-Boltzmann law, we have the local effective temperature on the disk expressed by

$$T_{\text{d}}(r) = (F_{\text{d}}/\sigma_{\text{SB}})^{1/4}, \quad (7)$$

where σ_{SB} is the Stefan-Boltzmann constant. The local radiation spectrum is defined by the Planck function:

$$B_{\nu}(r) = \frac{2h}{c^2} \frac{v^3}{\exp[hv/k_{\text{B}}T_{\text{d}}(r)] - 1}. \quad (8)$$

Thus the multicolor black-body spectrum of the disk is

$$L_{\nu} = \int_{r_{\text{in}}}^{r_{\text{out}}} B_{\nu}(r) 2\pi r dr. \quad (9)$$

3.2. Monte Carlo simulation

If the disk is covered by a corona, we need to resolve the radiative transfer in the hot corona to get the emergent spectrum. Radiative transfer has been computed in different ways. One approach is to solve the radiative transfer equation either numerically or analytically (e.g. Sunyaev & Titarchuk 1980; Poutanen & Svensson 1996). Another is the Monte Carlo simulation (e.g. Pozdnyakov et al. 1983, hereafter P83; Gorecki & Wilczewski 1984; GF91; Stern et al. 1995; Hua 1997, hereafter H97; Yao et al. 2005). The emergent spectrum can also be obtained by some approximate semi-analytical formulae (e.g. Zdziarski 1986; Hua & Titarchuk 1995). In this paper we calculate the spectrum by using the Monte Carlo simulation.

Compared with H97, photon absorption in the disk is taken into account in our model, which makes the simulation slightly more complex. The steps in the simulation are: (i) sample a seed photon including its position, energy, and direction; (ii) randomly choose a value for its free path and test whether it can leave the disk or corona; (iii) simulate the interaction of the photon with the medium; (iv) repeat steps (ii), (iii) till the photon leaves the system of the corona and disk.

3.2.1. Sampling the seed photons

The probability density of the seed photon can be written as

$$p(r, v) = 2\pi r dr \cdot F_{\nu}(r)/L, \quad (10)$$

where $F_{\nu}(r)$ is the flux density at r , $L \equiv \int_{r_{\text{in}}}^{r_{\text{out}}} L(r) dr$ is the total luminosity of the disk, and $L(r) dr = 2\pi r F_{\text{d}}(r) dr$ is the luminosity of the ring $r \sim r + dr$. Obviously, $p(r, v)$ can be expressed as follows,

$$p(r, v) = \frac{L(r) dr}{L} \cdot \frac{2\pi r \cdot F_{\nu}(r) dr}{L(r) dr} = \frac{L(r) dr}{L} \cdot \frac{F_{\nu}(r)}{F_{\text{d}}(r)} = \tilde{p}(r) B_{\nu}(r) \quad (11)$$

where $\tilde{p}(r)$ is the probability of a photon emitted in the ring $r \sim r + dr$, which can be sampled by tabulation. The Planck function $B_{\nu}(r)$ can be sampled as described in P83.

3.2.2. Drawing the free path

For the photon scattered in the corona, the probability of its travelling at least an optical depth τ is $e^{-\tau}$, so the optical depth that the photon travels between the i th and $(i+1)$ th scatterings can be drawn with $\tau_i = -\ln \lambda$, where $0 \leq \lambda \leq 1$ is a random number corresponding to a random event. Then the free path of the photon can be drawn with $\frac{\tau_i}{n_e \sigma} = \frac{-\ln \lambda}{\sigma} \cdot \frac{\sigma_{\text{T}} H_c}{\tau_c}$, where n_e , σ , and $\sigma_{\text{T}} = 6.65 \times 10^{-24} \text{ cm}^2$ are the number density of the electrons, cross-sections of scattering, and Thomson scattering, respectively. The parameters H_c and τ_c are the vertical height and optical depth of the corona, respectively. Because the corona is very hot, electrons in it are relativistic, which means that σ depends not only on the energy of the photon but also on the energy and direction of the electron, so the cross-section averaged over the distribution of the electrons in H97 is used to draw the free path of the photon.

Since the disk is assumed to be ‘‘cold’’, with hydrogen and helium fully ionized and all other elements neutral or weakly ionized, hard X-ray photons irradiating the disk from the corona can be absorbed by the atoms and scattered by the free electrons.

In this case, there are two viable ways to draw the free path of the photon: (i) choose the lesser of the two free paths that are drawn with σ_a and σ_s (GF91), where σ_a and σ_s are the cross sections of absorption and scattering, respectively; (ii) draw the free path with $\sqrt{\sigma_a(\sigma_a + \sigma_s)}$ and determine the interaction by drawing a random number λ and comparing it with the probability that a free path ends with absorption, i.e., $\zeta = \frac{\sigma_a}{\sigma_a + \sigma_s}$. If $\lambda \leq \zeta$, the photon will be absorbed and otherwise be scattered (Rybicki & Lightman 1979). We follow the first way in our simulations. Since electrons in the disk are nonrelativistic, σ_s can be given by the Klein-Nishina formula:

$$\sigma_s = \frac{3\sigma_T}{4} \cdot \frac{1}{x} \times \left[\left(1 - \frac{4}{x} - \frac{8}{x^2} \right) \ln(1+x) + \frac{1}{2} + \frac{8}{x} - \frac{1}{2(1+x)^2} \right], \quad (12)$$

where $x = 2h\nu/m_e c^2$ is the energy of the incident photon in units of electron-rest-energy. The cross section of absorption σ_a is taken from Morrison & McCammon (1983).

As the free path is known, the position where the photon arrives before the next interaction can be calculated. If the photon is outside the corona-disk system, it will escape the system, and its energy and direction are recorded. But if the photon transfers from the disk to the corona or the inverse, the point where the trajectory of the photon crosses the interface between the disk and corona should be regarded as the next initial position of the photon in calculations (see H97 for details).

3.2.3. Simulating the interaction

If the photon is scattered in the corona or disk, we can first sample an electron from thermal distribution, and then calculate the energy and direction of the scattered photon following the procedure described in P83.

The bound-free absorption of hard X-rays by the atoms in the disk will lead to ionization and vacancy, and will induce emission of fluorescence lines with the probability called fluorescence yield, Y , rather than ejection of Auger electrons. In the simulations, if the photon is absorbed by a certain atom or ion, we can draw a random number λ ($0 \leq \lambda \leq 1$) and compare it to the corresponding fluorescence yield. If $\lambda < Y$, an emission line emerges, whose direction can be sampled from the isotropic distribution. If $\lambda > Y$, an Auger electron is sent out, the photon vanishes, and its trajectory ends.

Because of the large abundance and cross-section of iron absorption, only the 6.4 keV Fe $K\alpha$ fluorescence line is considered in our simulations. If the energy of the absorbed photon is less than the iron K-shell absorption edge, i.e. $E < 7.1$ keV, no emission line is produced, while Fe $K\alpha$ lines emanate with $Y = 0.34$ for $E > 7.1$ keV.

3.3. Parameters of the corona and simulation results

Optically thin, thermal Compton-scattering spectra are well represented by power laws with exponential cut-offs, and the spectral index can be approximately given by (e.g. Rybicki & Lightman 1979)

$$\alpha = -\frac{\ln P}{\ln A_1}. \quad (13)$$

In Eq. (13) $A_1 = 1 + 4\Theta + 16\Theta^2$ is the average photon energy amplification per scattering, where $\Theta = kT_c/m_e c^2$ with T_c the

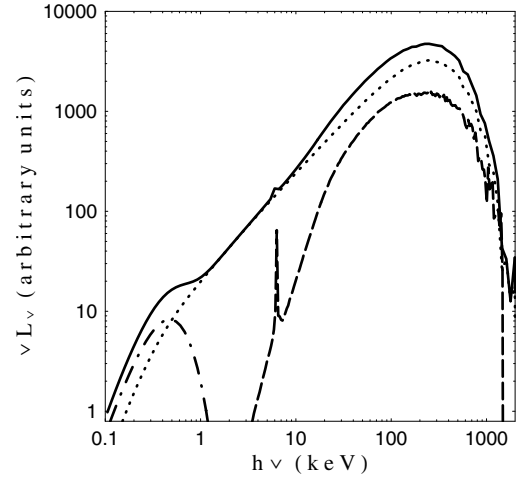


Fig. 2. The spectrum of the disk-corona system (solid line) and its components. The black-body, power-law, and reflected components are shown in dot-dashed, dotted, and dashed lines, respectively. The parameters $a_* = 0.998$, $n = 3$, and $B = 10^6$ G are taken.

coronal temperature. The average scattering probability P for a uniform slab is given by Zdziarski et al. (1994) as

$$P = 1 + \frac{\exp(-\tau)}{2} \left(\frac{1}{\tau} - 1 \right) - \frac{1}{2\tau} + \frac{\tau}{2} E_1(\tau), \quad (14)$$

where E_1 is the exponential integral (Press et al. 1992).

Observations of Seyfert galaxies show that their spectral indexes and the coronal Thomson optical depths are about 0.9 and 1, respectively (HM91; Zdziarski 1998), so we take $\alpha = 0.9$, $\tau = 1$ in our simulations. From Eq. (13), we estimate the temperature of the corona to be $T_c \approx 60$ keV.

In the following calculations, the radii of the inner and outer edges of the corona and disk are taken as r_{ms} and $20r_{ms}$, respectively. The half heights of the disk and the corona are assumed to be $H_d = 0.02r_{ms}$ and $H_c = r_{ms}$, respectively. The value of $H_d \ll r_{ms}$ does not affect the final results. The radial range of the disk is taken to be rather small, because the MC power concentrates in the innermost region of the disk, and it can be easily verified that at least 80% of the radiation is emanated within $20r_{ms}$.

Since the typical magnetic field of the supermassive and stellar BHs are about 10^4 G and 10^8 G, respectively, we take the middle value, 10^6 G, in simulations. A large number (10^9) of photons are traced to get one spectrum in simulations, and the result of 10^9 events costs about 100 min in running the program on a PC with a 2.8 GHz Pentium 4 CPU. All the spectra in this paper are given in forms of curves rather than histograms to make the curves look smooth.

The simulation results are given in Fig. 2. The spectrum of the disk-corona system comprises three components: the black-body spectrum formed by unscattered photons, the power-law spectrum formed by photons that escape from the corona after several times of inverse Compton scatterings, and the reflected spectrum characterized by iron fluorescence line and reflection hump.

In order to study the effects of the MC process and corona, the spectra of the disk-corona system with and without the MC process and those with and without corona are simulated as shown in Fig. 3. From this figure we find: (i) the disk can at most emit soft X-rays with $E < a$ few keV without corona, while the spectrum becomes much more complex and much harder when a corona exists; (ii) the MC process can increase the flux and

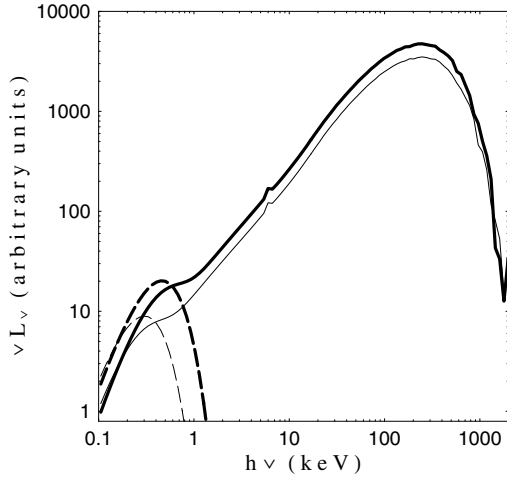


Fig. 3. Multicolor spectra of the disk and the simulated spectra of the disk-corona system. Thick and thin lines correspond to the spectra with and without the MC process, respectively. Solid and dashed lines correspond to the spectra with and without a corona, respectively. The parameters $a_* = 0.998$, $n = 3$, and $B = 10^6$ G are taken.

extend the spectrum to higher energy when the corona does not exist, but it can only augment the flux and has no influence on the cutoff energy and the index of the spectrum.

That the cutoff energy and index of the spectrum are indifferent to the MC process when a corona exists is because the spectral cutoff $h\nu_{\text{cut}}$ and index α are determined by Θ and τ , which are independent of the MC process in our model. Spectra with different a_* , n , and B are given in Fig. 4, from which we find (i) the fluxes increase with a_* and B whether the MC process exists or not; (ii) the parameter n has little influence on the flux.

It can be easily explained why the fluxes increase with a_* and B whether the MC process exists or not. For pure accretion without the MC process, as a_* increases, the inner edge of disk approaches the BH horizon, and more gravitational energy can be released if the accretion rate is the same, so the fluxes of the disk-corona system increase with a_* . According to Eq. (5), a stronger magnetic field corresponds to a higher accretion rate \dot{M}_D , and thus to higher fluxes. In the presence of the MC process, higher fluxes are produced for higher a_* and B since the MC power increases with both a_* and B . The flux is almost unaffected by n because the MC power is not significantly affected by n .

4. Application to astrophysics

As we introduce corona into our model, the radiative features of the BH accretion disk change significantly, and the X-ray spectra with hard X-rays can be simulated naturally for the given corona parameters. Compared with our previous model, this model provides more reasonable explanations for the observations involving X-ray band, such as the powers of 3C 273 in radio and X-ray bands, a very steep emissivity in the Seyfert 1 galaxy MCG-6-30-15, and quasi-periodic oscillations (QPOs) in the BH binaries.

4.1. Jet

The same as for our previous model, the BZ and MC processes can coexist in the present model, provided that parameters a_* and n are greater than some critical values, and their powers are

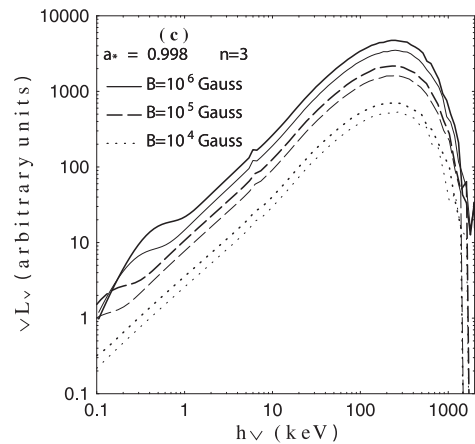
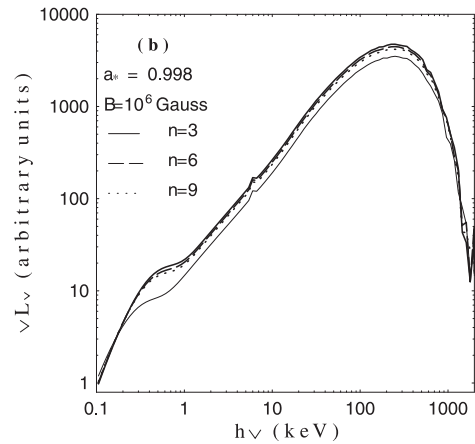
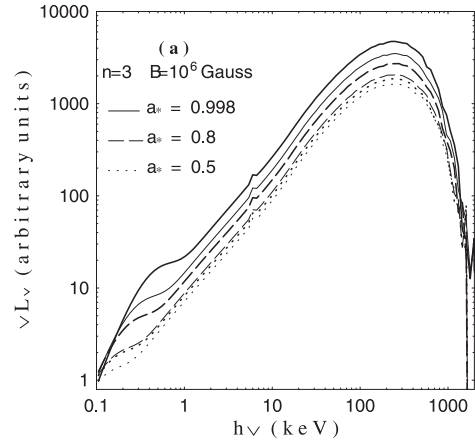


Fig. 4. Spectra corresponding to different values of the parameters a_* , n , and B in **a)**, **b)**, and **c)**, respectively. Thick lines correspond to states with the MC process, and thin ones to those without it.

derived by using a modified equivalent circuit and expressed as follows (W03b),

$$P_{\text{BZ}}/P_0 = 2a_*^2 \int_0^{\theta_M} \frac{k(1-k) \sin^3 \theta d\theta}{2 - (1-q) \sin^2 \theta}, \quad 0 < \theta < \theta_M, \quad (15)$$

$$P_{\text{MC}}/P_0 = 2a_*^2 \int_{\theta_M}^{\theta_L} \frac{\beta(1-\beta) \sin^3 \theta d\theta}{2 - (1-q) \sin^2 \theta}, \quad \theta_M < \theta < \theta_L, \quad (16)$$

where $P_0 \equiv (B_H^p)^2 M^2$.

An important feature of our model is that the strength of the BZ power relative to the MC power can be adjusted by virtue of

the angle θ_M , which is the angular boundary between the open and closed field lines at the BH horizon as shown in Fig. 1. As argued in W03b, θ_M is eventually determined by the parameters a_* and n contained in the mapping relation between the angular coordinate on the BH horizon and the radial coordinate on the disk.

Combining accretion with the MC process, the luminosity of the disk can be expressed as

$$L = (1 - E_{\text{ms}})\dot{M}_D + P_{\text{MC}}. \quad (17)$$

The first term in Eq. (17) comes from disk accretion, and the second term from the contribution of the MC process. The quantity E_{ms} is the specific energy of the accreting matter corresponding to the marginally stable orbit, which reads (Novikov & Thorne 1973)

$$E_{\text{ms}} = \frac{(1 - 2\chi_{\text{ms}}^{-2} + a_*\chi_{\text{ms}}^{-3})}{(1 - 3\chi_{\text{ms}}^{-2} + 2a_*\chi_{\text{ms}}^{-3})^{1/2}}. \quad (18)$$

Our model can be applied to the observations of some sources, by fitting the jet power in the radio band driven by the BZ process and fitting the bolometric luminosity driven by disk accretion and the MC process. Here we apply our model to fit the observational data of 3C 273. The BH mass contained is estimated as $6.59 \times 10^9 M_\odot$ by the reverberation method, the bolometric luminosity L is estimated to be $\sim 10^{47} \text{ erg s}^{-1}$ (Paltani & Türler 2005), and the minimum jet power is given as $P_{\text{jet}}^{\text{min}} = 6.61 \times 10^{45} \text{ erg s}^{-1}$ (Celotti et al. 1997). If the magnetic field at the BH horizon is considered to be $B_{\text{H}}^p \approx 10^4 M_9^{-1/2} \text{ G}$ (Beskin 1997), we can estimate some parameters of our model as $a_* \approx 0.76$, $n \approx 6.13$, and $\theta_M \approx 48^\circ$ by combining Eqs. (15)–(18) with the relation (5).

The spectral index, $\alpha \approx 0.77$, and luminosity of the X-rays in the range of 3–10 keV, $L_{3-10} \approx 0.81 \times 10^{46} \text{ erg s}^{-1}$ can be derived from Page et al. (2004), where some X-ray observational results of 3C 273 are listed. Combining Eq. (13) with the assumption that $\tau = 1$, we have $T_c \approx 73 \text{ keV}$. Using the Monte Carlo method we find that $L_{3-10} \approx 0.72 \times 10^{46} \text{ erg s}^{-1}$, which is only a little less than the observational data. Since 3C 273 is a well known radio-loud quasar with a jet showing superluminal motion, the X-rays emitted by synchrotron self-Comptonization of high-energy electrons in the jet should be considered. Moreover, the degree of the ionization of the disk is supposed to be low in our model, which means higher absorption in the range $\sim 10 \text{ keV}$. If these reasons are considered, the luminosity of the X-rays could be fitted well with our model.

4.2. Steep emissivity index

Wilms et al. (2001) assume that the reflected flux has an emissivity profile $\propto r^{-\beta}$ in fitting the 2–10 keV observational data of the Seyfert I galaxy MCG-6-30-15, and found a very interesting result. The emissivity profile is very steep with $\beta = 4.3\text{--}5.0$, which is too high to be explained by the standard accretion disk model.

In W03a and W03b, we explained the very steep emissivity profile by the local radiation flux emitted in a black-body spectrum by virtue of the MC process. However, the spectra of previous models cannot extend to $\sim 10 \text{ keV}$ for AGNs, which is not consistent with the observations. This inconsistency can be removed in the MC model with corona.

Taking Fe $K\alpha$ fluorescence as an example, we find in Fig. 5 that the photon numbers produced in our model reduce more quickly with the disk radius than those produced in the standard

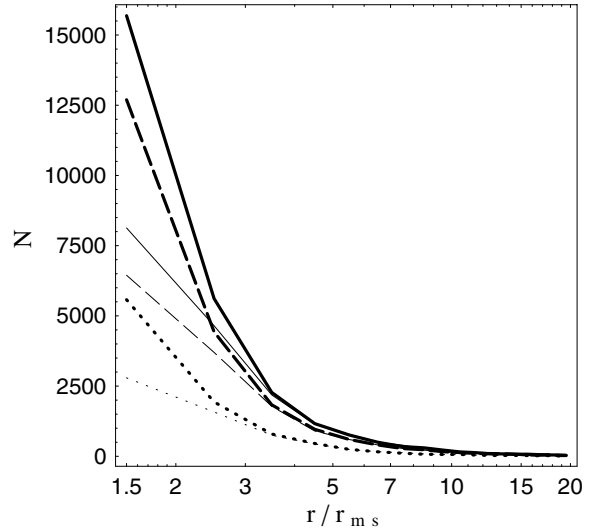


Fig. 5. The numbers of iron fluorescence photons at different radii and different incline angles. Solid lines, dashed lines, and dotted lines correspond to $\mu = \cos i = 0.95, 0.75, 0.35$, respectively. Thick lines correspond to states with the MC process, and thin ones to those without it. The parameters, $a_* = 0.998$, $n = 3$, and $B = 10^6 \text{ G}$ are given.

disk with corona. It turns out that the very steep emissivity produced in the MC process could not be changed by the presence of the corona.

4.3. QPOs

Wang et al. (2003c) explained QPOs by virtue of rotating hotspots arising from non-axisymmetric magnetic fields. When a corona is introduced into our model, although the rotational energy of the BH is shared by the disk and the corona (i.e., the temperature of the hotspot on the disk decreases), the total flux from the region of higher magnetic field remains unchanged. As a result, as the high-magnetic-field region rotates, the fittings to the frequency of the QPOs are still valid. An interesting phenomenon that is different from the previous model is that we cannot see a hotter spot in the corona because of the cooling of more soft photons from the disk. Additionally, the introduction of corona into our model is helpful for interpreting QPOs, which are usually observed in the steep power-law state (McClintock & Remillard 2003).

Although the introduction of the corona into our model is helpful for fitting the observations, our model needs to be improved in some aspects. For example, more reasonable geometry and parameters of the corona should be adopted (e.g. Haardt et al. 1994; Liu et al. 2002), the cooling of synchrotron radiation should be considered, and gravitational effects on the trajectories of photons need to be taken into account since they cannot be ignored in the inner region of the disk around a rapidly spinning BH. We shall deal with these problems in future works.

Acknowledgements. This work is supported by the National Natural Science Foundation of China under Grant Numbers 10373006, 10573006, and 10121503. The anonymous referee is thanked for helpful comments and suggestions for improving our manuscript. R.Y.M. would like to thank Dr. B. F. Liu and Dr. Y. S. Yao for helpful discussions.

References

- Beskin, V. S. 1997, *Physics Uspekhi*, 40, 659
- Blandford, R. D. 1999, in *Astrophysical Discs*, ed. J. A. Sellwood, & J. Goodman, ASP Conf. Ser., 160, 265 [arXiv:astro-ph/9902001]

- Blandford, R. D. 2002, Lighthouses of the Universe: The Most Luminous Celestial Objects and Their Use for Cosmology Proceedings of the MPA/ESO/, 381 [arXiv:astro-ph/0202265]
- Cao, X. W. 2004, ApJ, 613, 716
- Celotti, A., Padovani, P., & Ghisellini, G. 1997, MNRAS, 286, 415
- Di Matteo, T., Celotti, A., & Fabian, A. C. 1997, MNRAS, 291, 805
- Esin, A. A. 1999, ApJ, 517, 381
- Field, G. B., & Rogers, R. D. 1993, ApJ, 403, 94
- Galeev, A. A., Rosner, R., & Vaiana, G. S. 1979, ApJ, 219, 318
- Galbiati, E., Caccianiga, A., Maccacaro, T., et al. 2005, A&A, 430, 927
- George, I. M., & Fabian, A. C. 1991, MNRAS, 249, 352 (GF91)
- Ghisellini, G., Haardt, F., & Svensson, R. 1998, MNRAS, 297, 348
- Gorecki, A., & Wilczewski, W. 1984, Acta Astron., 34, 141
- Haardt, F., & Maraschi, L. 1991, ApJ, 380, L51 (HM91)
- Haardt, F., & Maraschi, L. 1993, ApJ, 413, 507
- Haardt, F., Maraschi, L., & Ghisellini, G. 1994, ApJ, 432, L95
- Hua, X. M. 1997, Computers in Physics, 11, 660 (H97)
- Hua, X. M., & Titarchuk, L. G. 1995, ApJ, 449, 188
- Li, L. X. 2002a, ApJ, 567, 463
- Li, L. X. 2002b, A&A, 392, 469
- Li, L. X., & Paczynski, B. 2000, ApJ, 534, L197
- Liang, E. P. 1998, Phys. Rep., 302, 67
- Liang, E. P., & Price, R. H. 1977, ApJ, 218, 247
- Liu, B. F., Mineshige, S., & Shibata, K. 2002, ApJ, 572, L173
- Livio, M., Ogilvie, G. I., & Pringle, J. E. 1999, ApJ, 512, 100
- Macdonald, D., & Thorne, K. S. 1982, MNRAS, 198, 345
- McClintock, J. E., & Remillard, R. A. 2003 [arXiv:astro-ph/0306213]
- Merloni, A., & Fabian, A. C. 2002, MNRAS, 332, 165
- Miller, J. M., Fabian, A. C., Wijnands, R., et al. 2002, ApJ, 570, 69
- Moderski, R., Sikora, M., & Lasota, J. P. 1997, in Proceedings of the International Conf., Relativistic Jets in AGNs, ed. M. Ostrowski, M. Sikora, G. Madejski, & M. Begelman, 110 [arXiv:astro-ph/9706263]
- Morrison, R., & McCammon, D. 1983, ApJ, 270, 119
- Novikov, I. D., & Thorne, K. S. 1973, in Black Holes – Les Astres Occlus, ed. C. DeWitt, & B. DeWitt (New York, London: Gordon and Breach), 345
- Page, D. N., & Thorne, K. S. 1974, ApJ, 191, 499
- Page, K. L., Turner, M. J. L., Done, C., et al. 2004, MNRAS, 349, 57
- Paltani, S., & Türler, M. 2005, A&A, 435, 811
- Poutanen, J., & Svensson, R. 1996, ApJ, 470, 249
- Pozdnyakov, L. A., Sobol, I. M., & Sunyaev, R. A. 1983, Ap&SS Rev., 2, 189, 83 (P83)
- Press, W. H., Teukolsky, S. A., Vetterling, W. T., et al. 1992, in Numerical Recipes, 2nd ed. (Cambridge: Cambridge Univ. Press)
- Rybicki, G. B., & Lightman, A. P. 1979, in Radiative Processes in Astrophysics (New York: Wiley Interscience)
- Stern, B. E., Begelman, M. C., Sikora, M., et al. 1995, MNRAS, 272, 291
- Sunyaev, R. A., & Titarchuk, L. G. 1980, A&A, 86, 121
- Thorne, K. S., Price, R. H., & Macdonald, D. A. 1986, in Black Holes: The Membrane Paradigm (Yale University Press)
- Tout, C. A., & Pringle, J. E. 1996, MNRAS, 281, 219
- van Putten, M. H. P. M. 1999, Science, 284, 115
- Wang, D. X., Xiao, K., & Lei, W. H. 2002, MNRAS, 335, 655
- Wang, D. X., Lei, W. H., & Ma, R. Y. 2003a, MNRAS, 342, 851 (W03a)
- Wang, D. X., Ma, R. Y., Lei, W. H., et al. 2003b, ApJ, 595, 109 (W03b)
- Wang, D. X., Ma, R. Y., Lei, W. H., et al. 2003c, MNRAS, 344, 473
- Wilms, J., Reynolds, C. S., Begelman, M. C., et al. 2001, MNRAS, 328, L27
- Yao, Y. S., Zhang, S. N., Zhang, X. L., et al. 2005, ApJ, 619, 455
- Zdziarski, A. A. 1986, ApJ, 303, 94
- Zdziarski, A. A. 1998, MNRAS, 296, L51
- Zdziarski, A. A., Fabian, A. C., Nandra, K., et al. 1994, MNRAS, 269, L55
- Zhang, S. N., Cui, W., Chen, W., et al. 2000, Science, 287, 1239